Self-Assembled Ionophores from Isoguanosine

Jeffery T. Davis,*,† Sampath Tirumala,† James R. Jenssen,† Eric Radler,† and Dan Fabris‡

Department of Chemistry and Biochemistry, University of Maryland, College Park, Maryland 20742 and Department of Chemistry and Biochemistry, University of Maryland, Baltimore County, 5401 Wilkens Avenue, Baltimore, Maryland 21228

Received December 12, 1994 (Revised Manuscript Received April 18, 1995⊗)

The isoguanosine (isoG) mononucleoside **3** forms a C_4-symmetric tetramer in organic solvents. The isoG tetramer **6** has been characterized by 2D NMR spectroscopy, UV spectroscopy, and FAB mass spectrometry. Specific NOEs between the exocyclic C6NH$_2$ amino protons and the ribose H1′ and H2′ protons confirmed the isoG self-association and was the basis for the tetramer model. Molecular models of isoG dimers, trimers, and tetramers show that only the C_4-symmetric tetramer **6** is consistent with the observed NH6-H1′, H2′ NOEs. In the isoG tetramer, hydrogen bonds between C6NH$_A$ and a purine N3 bring both exocyclic amino protons within 3–4 Å of the adjacent monomer's ribose H1′ and H2′ protons. The isoG tetramer **6** organizes by hydrogen bonding between the Watson–Crick face of one isoG base and the complementary bottom edge of another purine. The tetramer is stabilized by an inner and outer ring of hydrogen bonds. The inner ring forms between the imino NH1 proton of one monomer and the C2 carbonyl oxygen of an adjacent monomer, while the outer ring is made up of four NH6–N3 hydrogen bonds. The isoG tetramer is thermodynamically very stable, with a K_s of ca. 10^9–10^{10} M^{-3} at room temperature, and a $\Delta G°$ of tetramer formation of −12.5 kcal mol^{-1} in d_6-acetone at 25 °C. The van't Hoff plots indicated that the thermodynamic parameters for tetramer formation were $\Delta H° = -18.2$ kcal mol^{-1} and $\Delta S°_{298} = -19.1$ eu. Each isoG C2 oxygen in the tetramer has a nonbonded electron pair that points into a central cavity, enabling selective cation coordination. Solutions of the isoG mononucleoside **3** in d_6-acetone were titrated with LiCl, NaI, KI, and BaI$_2$. Each of these ions had a dramatic effect on the isoG structural equilibrium. Thus, Li$^+$ destabilized the tetramer and shifted the equilibrium back to the monomer. Low concentrations of Na$^+$, on the other hand, stabilized the tetramer. Titrations of solutions of isoG **3** with the larger cations, K$^+$ and Ba^{+2}, indicated that 1 equiv of metal coordinated 8 nucleotide monomers, suggesting formation of a metal-stabilized octamer. The NMR analysis indicates that the isoG-K$^+$ tetramer **6** is much more stable than the corresponding guanosine-K$^+$ complex.

Introduction

Ion complexation is fundamental to many chemical and biological processes, and thousands of natural and synthetic ionophores have been described.[1] Usually, covalent bonds constrain the ionophore into a preorganized conformation for productive ion binding. Classic examples include crown ethers and cryptands.[2] An alternative design involves the use of noncovalent interactions to build a host molecule. Recent reports describe the use of noncovalent interactions to form molecular self-assemblies that bind alkali cations.[3] One of our current research goals is to use hydrogen bonds to construct multidentate cation-binding ligands (Scheme 1).

Scheme 1

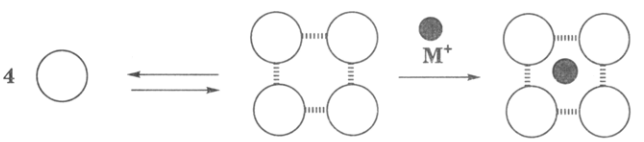

A self-assembled ionophore may have advantages over covalent chelators. For example, it is often difficult to recover a metal ion from its ionophore complex because of the high stability constants.[4] An ionophore that is held together by hydrogen bonds, however, should release the cation on addition of a protic solvent to a nonprotic organic solution of its metal complex. Self-assembled ionophores, therefore, may find applications in the purification of rare earth metals and radioactive isotopes.[5]

Nature provides many examples of organized structures performing specific functions. This project's inspiration comes from nucleic acid structures containing the G-quartet (**1**).[6] The G-quartet (**1**) is a noncovalent assembly of four Hoogsteen paired guanines with a central cavity containing four oxygens that can coordinate cations via ion–dipole interactions. It is well-known that stabilization of G-quartet structures depends on the

* Author to whom correspondence should be addressed.
† University of Maryland—College Park.
‡ University of Maryland—Baltimore County.
⊗ Abstract published in *Advance ACS Abstracts,* June 15, 1995.

(1) Izatt, R. M.; Pawlak, K.; Bradshaw, J. S.; Bruening, R. L. *Chem. Rev.* **1991**, *91*, 1721.
(2) Gokel, G. *Crown Ethers and Cryptands*; Royal Society of Chemistry: Cambridge, England; 1991; p 105.
(3) (a) Schepartz, A.; McDevitt J. P. *J. Am. Chem. Soc.* **1989**, *111*, 5976. (b) Schall, O. F.; Robinson, K.; Atwood, J. L.; Gokel, G. W. *J. Am. Chem. Soc.* **1993**, *115*, 5962. (c) Bell, T. W.; Jousselin, H. *Nature* **1994**, *367*, 441.
(4) (a) Pedersen, C. J. *J. Am. Chem. Soc.* **1967**, *89*, 7017. (b) Horwitz, E. P.; Dietz, M. L.; Fisher, D. E. *Solvent Extraction and Ion Exchange* **1991**, *9*, 1; (c) Chiarizin, R.; Horwitz, E. P.; Dietz, M. L. *Solvent Extr. Ion Exch.* **1992**, *10*, 337. (d) Du, H. S.; Wood, D. J.; Elshani, S.; Wai, C. M. *Talanta* **1993**, *40*, 173.
(5) (a) Zhangyu, Y.; Ranqi, K.; Men, Q.; Binghan, W.; Bin, Z. *J. Chem. Soc., Chem. Commun.* **1994**, 1753. (b) Nakagawa, K.; Inoue, Y.; Hakushi, T. *J. Chem. Soc., Chem. Commun.* **1991**, 1683.
(6) (a) Williamson, J. R., Raghuraman, M. K., Cech, T. R. *Cell* **1989**, 871. (b) Sundquist, W. I.; Klug, A., *Nature* **1989**, *342*, 825. (c) Sen, D.; Gilbert, W. *Nature* **1988**, *334*, 364. (d) Blackburn, E. H. *Annu. Rev. Biochem.* **1992**, *61*, 113. (e) Sen, D.; Gilbert, W. *Methods Enzymol.* **1992**, *211*, 191.

0022-3263/95/1960-4167$09.00/0

radius and charge of the cation.[7] Molecules ranging from guanine mononucleotides[8] to poly(guanylic acid)[9] to DNA and RNA oligonucleotides[10] form G-quartets.

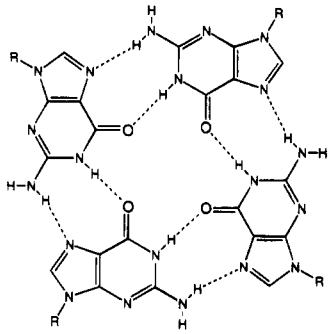

G-Quartet 1

Analysis of the G-quartet structure suggested that modified nucleosides, with different hydrogen bonding patterns, might form self-assemblies even more stable than the native G-quartet. The first candidate that we studied was isoguanosine **2** (isoG), a C-2 oxidized adenosine. IsoG differs from G in that the carbonyl and amine at the purine's C-2 and C-6 positions are transposed. In this paper, we demonstrate that this simple change in hydrogen-bond donor and acceptor sites has dramatic consequences in stabilizing a self-associated isoG complex relative to the corresponding G complex.

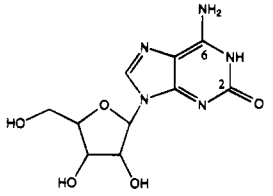

IsoG 2

IsoG, or its analogs, have been isolated from plants,[11] butterflies,[12] and mollusks.[13] In addition, isoG is a significant DNA oxidation product in Ni(II) and Co(II)-treated human chromatin.[14] IsoG is also an essential constituent of a Cu(II) containing ribonucleopeptide produced by cultured pig macrophages.[15] This unusual, extracellular RNA has been reported to be a potent angiogenesis factor. IsoG, or analogs, also stimulate cyclic-AMP accumulation in the brain,[16] inhibit IMP pyrophosphorylase,[17] and act as adenosine A_1-receptor agonists.[18]

IsoG's hydrogen bonding pattern undoubtly contributes to its unique physical and biological properties. For example, poly(isoguanylic acid) forms highly-organized gels in H_2O.[19,20] Spectrocopic studies showed that the poly(isoG)'s secondary structure was even stronger than that in poly(G) helices. A C_2-symmetric, hydrogen-bonded tetramer was proposed as the basic unit for the four-stranded poly(isoG) helix.[20] Recently, there has been a flurry of reports concerning the use of isoG to study nucleic acid structure and function. The groups of Benner,[21] Seela,[22] Eckstein,[23] Dervan,[24] and Eschenmoser[25] have incorporated isoG analogs into oligonucleotides in order to study its pairing with natural and unnatural bases.

This paper describes our initial studies on the self-association of the protected isoG **3**. The present study demonstrates that this isoG mononucleoside forms extraordinarily stable supramolecular structures, even in organic solvents of relatively high dielectric constant. NMR experiments indicate that the isoG mononucleoside **3** associates to give a C_4-symmetric hydrogen-bonded tetramer. The isoG tetramer is a self-assembled ionophore that, in turn, selectively coordinates monovalent and divalent cations to give extraordinarily stable complexes.

Preparation of Protected IsoG Derivative 3. Isoguanosine (**2**) was synthesized from 5-amino-1-(β-D-ribofuranosyl)imidazole-4-carboxamide according to the method of Chern and Townsend.[26] The Chern protocol, which can easily be done on a 25 g scale, is more convenient than the photochemical preparation of isoG from adenosine *N*-1-oxide.[27] We, first, wanted to compare, at the mononucleoside level, the hydrogen bond

(7) (a) Ross, W. S.; Hardin, C. C., *J. Am. Chem. Soc.* **1994**, *116*, 6070. (b) Hardin, C. C.; Henderson, E.; Watson, T.; Bailey, C. *Biochemistry* **1992**, *31*, 833.

(8) (a) Miles, H. T.; Frazier, J. *Biochem. Biophys. Res. Commun.* **1972**, *49*, 199. (b) Pinnavaia, T. J.; Marshall, C. L.; Mettler, C. M.; Fisk, C. L.; Miles, H. T.; Becker, E. D. *J. Am. Chem. Soc.* **1978**, *100*, 3625. (c) Borzo, M.; Petellier, C.; Laszlo, P.; Paris, A. *J. Am. Chem. Soc.* **1980**, *102*, 1124. (d) Mariani, P., Mazabrad, C., Garbesi, A., Spada, G. P. *J. Am. Chem. Soc.* **1989**, *113*, 6369.

(9) (a) Gellert, M.; Lipsett, M. N.; Davies, D. R., *Proc. Natl. Acad. Sci.* **1962**, *48*, 2013. (b) Arnott, S.; Chandrasekaran, R.; Martilla, C. M. *Biochem. J.* **1974**, *141*, 537. (c) Zimmerman, S. B.; Cohen, G. H.; Davies, D. R. *J. Mol. Biol.* **1975**, *92*, 181.

(10) (a) Laughlan, G.; Murchie, A. I. H.; Norman, D. G.; Moore, M. H.; Moody, P. C. E.; Lilley, D.; Luisi, B. *Science* **1994**, *265*, 520. (b) Aboula-ela, F., Murchie, A. I. H., Norman, D. G.; Lilley, D. M. J. *J. Mol. Biol.* **1994**, *243*, 458. (c) Wang, K., McCurdy, S., Shae, R. G.; Swaminathan, S.; Bolton, P. H. *Biochemistry* **1993**, *32*, 1899. (d) Wang, Y.; Patel, D. J. *Biochemistry* **1992**, *31*, 8112. (e) Smith, F. W.; Feigon, J. *Nature* **1992**, *356*, 164. (f) Smith, F. W.; Feigon, J. *Biochemistry* **1993**, *32*, 8682. (g) Cheong, C.; Moore, P. B. *Biochemistry* **1992**, *31*, 8406. (h) Aboul-ela, F.; Murchie, A. I. H.; Lilley, D. M. J. *Nature* **1992**, *360*, 280. (i) Kang, C.; Zhang, X.; Ratliff, R.; Moyzis, R.; Rich, A., *Nature* **1992**, *356*, 126. (j) Huizenga, D. E.; Szostak, J. W. *Biochemistry* **1995**, *34*, 656. (k) Lauhon, C. T.; Szostak, J. W. *J. Am. Chem. Soc.* **1995**, *117*, 1246.

(11) Cherbuliez, E.; Berhard, K. *Helv. Chim. Acta* **1932**, *15*, 464.

(12) Pettit, G. R.; Ode, R. H.; Coomes, M. R.; Ode, S. L. *Lloydia* **1976**, *39*, 363.

(13) Fuhrman, F. A.; Fuhrman, G. J.; Nachman, R. J.; Mosher, H. S. *Science* **1981**, *212*, 557.

(14) Nackerdien, Z.; Kasprzak, K. S.; Rao, G.; Halliwell, B.; Dizdaroglu, M. *Cancer Res.* **1991**, *51*, 5837.

(15) (a) Wissler, J. H.; Kiesewetter, S.; Logemann, E.; Sprinzl, M.; Hellmeyer, L. M. G., Jr. *Biological Chemistry (Hoppe-Seyler)* **1988**, *369*, 948. (b) Wissler, J. H.; Kiesewetter, S.; Logemann, E.; Sprinzl, M.; Hellmeyer, L. M. G., Jr. *Biological Chemistry (Hoppe-Seyler)* **1989**, *370*, 975.

(16) Huang, M.; Shimizu, H.; Daly, J. W. *J. Med. Chem.* **1972**, *15*, 462.

(17) Hagen, C. *Biochim. Biophys. Acta* **1973**, *293*, 105.

(18) Liaw, Y.-C.; Chern, J.-W.; Lin, G.-S.; Wang, A. H.-J. *FEBS Lett.* **1992**, *297*, 4.

(19) Sepiol, J.; Kazmierczuk, Z.; Shugar, D., *Z. Naturforsch.* **1976**, 361.

(20) Golas, T.; Fikus, M.; Kazimierczuk, Z.; Shugar, D. *J. Eur. Biochem.* **1976**, *65*, 183.

(21) (a) Switzer, C.; Moroney, S. E.; Benner, S. A. *J. Am. Chem. Soc.* **1989**, *111*, 8322. (b) Piccirilli, J. A.; Krauch, T.; Moroney, S. E.; Benner, S. A. *Nature* **1990**, *343*, 33. (c) Switzer, C. Y.; Moroney, S. E.; Benner, S. A. *Biochemistry* **1993**, *32*, 10489. (d) Bain, J. D.; Switzer, C.; Chamberlin, A. R.; Benner, S. A. *Nature* **1992**, *356*, 537.

(22) (a) Kazimierczuk, Z.; Mertens, R.; Kawczynski, W.; Seela, F. *Helv. Chim. Acta* **1991**, *74*, 1742. (b) Seela, F.; Mertens, R.; Kazimierczuk, Z. *Helv. Chim. Acta* **1992**, *75*, 2298. (c) Seela, F.; Frolich, T. *Helv. Chim. Acta* **1994**, *77*, 399.

(23) (a) Tuschl, T.; Ng, M. M. P.; Pieken, W.; Benseler, F.; Eckstein, F. *Biochemistry* **1993**, *32*, 11658. (b) Ng, M. M. P.; Benseler, F.; Tuschl, T.; Eckstein, F. *Biochemistry* **1994**, *33*, 12119.

(24) Tor, Y.; Dervan, P. B. *J. Am. Chem. Soc.* **1993**, *115*, 4461.

(25) Eschenmoser, A. *Pure Appl. Chem.* **1993**, *65*, 1179.

(26) Chern, J.-W.; Lin, G.-S.; Chen, C.-S.; Townsend, L. B. *J. Org. Chem.* **1991**, *56*, 4213.

(27) Cramer, V. F.; Schlingloff, G. *Tetrahedron Lett.* **1964**, *32*, 3201.

Table 1. ^{1}H NMR Chemical Shifts for isoG 3

resonance	chemical shift (ppm)				
	d_6-DMSO	CD3OD	CDCl3	CD3CN	d_6-acetone
NH1	*b*	*b*	13.04	13.06	13.04
$NH6_A$	*b*	*b*	10.70	10.73	10.77
$NH6_B$	*b*	*b*	6.98	7.12	7.17
H8	7.89	8.00	7.47 (7.72)[c]	7.57 (7.70)[c]	7.66 (7.85)[c]
H1′	5.91	6.05	5.76 (5.94)	5.80 (5.86)	5.86 (6.02)
H2′	5.24	5.31	4.97 (5.02)	5.00 (5.19)	5.16 (5.32)
H3′	4.88	5.01	4.75 (4.85)	4.81 (4.86)	4.94 (5.01)
H4′	4.13	4.32	4.50 (4.32)	4.54 (4.26)	4.59 (4.27)
H5′	3.75	3.87	3.82 (nd)	3.93 (3.82)	4.00 (nd)
H5″	3.69	3.85	3.71 (nd)	3.73 (3.74)	3.88 (nd)
CH_3 A	1.51	1.60	1.78 (1.60)	1.79 (1.53)	1.85 (1.55)
CH_3 B	1.31	1.40	1.40 (1.34)	1.40 (1.45)	1.49 (1.35)
tBu	0.81	0.89	0.74 (0.82)	0.76 (0.81)	0.86 (0.81)
SiMe A	−0.03	0.05	−0.04	−0.02	0.04
SiMe B	−0.03	0.05	−0.07	−0.02	0.04

[a] All spectra are for a 10 mM sample of **3** at 298 K. Spectra were recorded at 500 MHz. [b] Exchangeable NH1 and C6NH2 resonances are exchange-broadened. [c] Values in parentheses correspond to the minor resonance set for the isoG monomer.

interactions and aggregation behavior of isoG and G. The use of ^{1}H, ^{13}C, and ^{15}N NMR spectroscopy to study base pairing of protected nucleosides in organic solvents is well established.[28] Thus, we prepared the three purine derivatives isoG **3**, A **4**, and G **5**. The preparation of the 5′-t-BDMS-2′,3′-acetonide isoG **3** from synthetic isoG **2** was straightforward. The adenosine (**4**) and guanosine (**5**) analogs were similarly prepared. Protection of the ribose 2′ and 3′ hydroxyls as the cyclic acetonide, and blocking of the 5′-OH with a *tert*-butyldimethylsilyl group provided purine derivatives that were soluble in organic solvents. Once protected, isoG's hydrogen bonding interactions could be studied over a wide range of temperatures and concentrations in solvents of varying dielectric constants. In addition, the derivatization prevented formation of competing hydrogen bonds from the ribose hydroxyl protons.

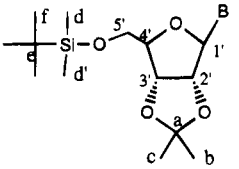

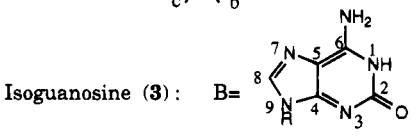

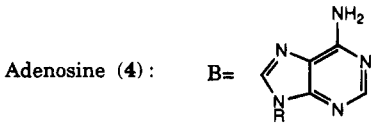

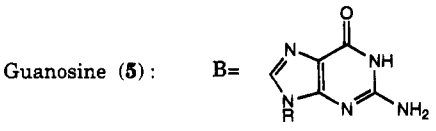

Evidence for IsoG Self-Association. The identity and purity of isoG **3** was confirmed by UV, IR, ^{1}H ,^{13}C, and ^{15}N NMR spectroscopies, and EI and FAB mass spectrometry. The 500 MHz ^{1}H NMR in d_6-DMSO or CD_3OD showed a single resonance for each of isoG's nonexchangeable protons. Because of chemical exchange, the nucleoside's three exchangeable NH protons are not observed in these polar solvents. The 125 MHz ^{13}C NMR spectrum in d_6-DMSO also showed a single set of resonances. While ^{1}H and ^{13}C NMR in the coordinating solvents d_6-DMSO and CD_3OD showed one set of resonances for isoG **3**, analyses in organic solvents of lower dielectric constants revealed a more complex structural equilibria. For example, two distinct sets of ^{1}H and ^{13}C NMR resonances, in slow exchange, were observed when **3** was dissolved in either $CDCl_3$, d_6-acetone, or CD_3CN (Tables 1 and 2). The equilibrium between the two sets of signals depends on the solvent polarity, the sample concentration, and the temperature, and it is diagnostic of a self-association process.

The ^{1}H and ^{13}C assignments for both sets of isoG resonances were determined from a series of ^{1}H−^{1}H COSY, ^{1}H−^{1}H NOESY, ^{1}H−^{1}H ROESY, ^{1}H−^{15}N HMQC and ^{1}H−^{13}C HMQC NMR correlation experiments. For example, the ^{1}H−^{1}H correlation (COSY) spectrum of a solution of **3** in $CDCl_3$ at room temperature clearly shows two different sets of cross peaks corresponding to the ribose's ^{1}H−^{1}H scalar couplings (Figure 1). Under these conditions, the two species exist in approximately a 2.5:1 ratio, with the major species having sharper ^{1}H resonances ($\Delta\nu$ = 1.5−2.0 Hz) than the minor resonance set ($\Delta\nu$ = 11.5−13.0 Hz). Similar COSY spectra were obtained in d_6-acetone and CD_3CN, although in these two solvents both species had similar lineshapes ($\Delta\nu$ = 1.5−2.0 Hz). The minor resonances in $CDCl_3$ were assigned to the isoG monomer **3** since both the ^{1}H and ^{13}C chemical shifts in $CDCl_3$ were similar to the chemical shifts observed in the coordinating solvent DMSO (Table 1). The major ^{1}H resonances in $CDCl_3$ were consistent with a single self-associated, hydrogen-bonded structure. Specifically, the ^{1}H−^{1}H NOESY and ^{1}H−^{15}N HMQC NMR experiments indicated that this major resonance set had three exchangeable and nitrogen-bound protons.

Resonance Assignments for Self-Associated IsoG. The isoG's two exocyclic amino protons, $C6NH_A$ and $C6NH_B$, and its N1 imino proton were identified from ^{1}H−^{15}N HMQC[29] and ^{1}H−^{1}H NOESY[30] NMR experiments. Identification of these three exchangeable pro-

(28) (a) Iwashashi, H; Kyogoku, Y. *J. Am. Chem. Soc.* **1977**, *99*, 7761. (b) Gmeiner, W. H.; Poulter, C. D., *J. Am. Chem. Soc.* **1988**, *110*, 7640. (c) Williams, N. G., Williams, L. D.; Shaw, B. R., *J. Am. Chem Soc.* **1990**, *112*, 829. (d) Gannett, P. M.; Sura, T. P. *Chem. Res. Toxicol.* **1993**, *6*, 690.

(29) Bax, A.; Subramanian, S. *J. Magn. Reson.* **1986**, *67*, 565.

(30) Kumar, A.; Wagner, G.; Ernst, R. R.; Wuthrich, K. *J. Am. Chem. Soc.* **1981**, *103*, 3654.

Table 2. ^{13}C NMR Chemical Shifts for IsoG 3[a]

solvent	C2	C4	C5	C6	C8	C1′	C2′	C3′	C4′	C5′	C_a	C_b	C_c	C_d	$C_{d'}$	C_e	C_f
$CDCl_3$[b]	157.4 (157.0)	152.0 (151.7)	110.4	151.4	137.1 (136.9)	93.0 (90.7)	85.0	81.4 (80.9)	88.9 (87.3)	63.4	114.2 (113.7)	nd	nd	nd	nd	nd	nd
d_6-DMSO	nd	nd	nd	nd	137.7	88.5	83.4	81.8	86.5	63.2	113.0	27.0	25.8	−5.5	−5.5	25.8	18.0
CD_3CN/KI[c]	159.2	153.2	111.8	152.2	138.5	92.9	86.5	81.9	89.2	64.0	114.6	27.3	25.2	−5.3	−5.4	26.2	18.9
d_6-acetone/KI[c]	159.1	153.1	111.7	152.1	138.4	92.6	86.4	81.7	89.1	64.0	114.5	25.2	27.3	−5.3	−5.5	26.2	18.8
d_6-acetone/NaI[c]	156.6	151.0	109.1	154.0	138.6	90.4	84.7	81.5	86.7	63.7	113.5	25.2	26.5	−5.4	−5.5	24.9	17.6

[a] All spectra were obtained at 125 MHz frequency. The ^{13}C resonances for carbons with bound protons (C2, C8, C1′–C5′, C_b–C_e) were assigned from 2D HMQC ^{13}C–^1H experiments at 125 MHz using inverse detection.[29] The ^{13}C resonances for carbons with no attached protons were correlated with literature compounds. [b] In $CDCl_3$, two separate ^{13}C resonances could be observed for some carbons. Values in parentheses represent the minor component's ^{13}C resonances. [c] In both d_6-acetone and CD_3CN, isoG **3** shows two sets of resonances, one for the monomer and one for the tetramer. A single set of peaks is present when either excess NaI or KI are added to these solutions.

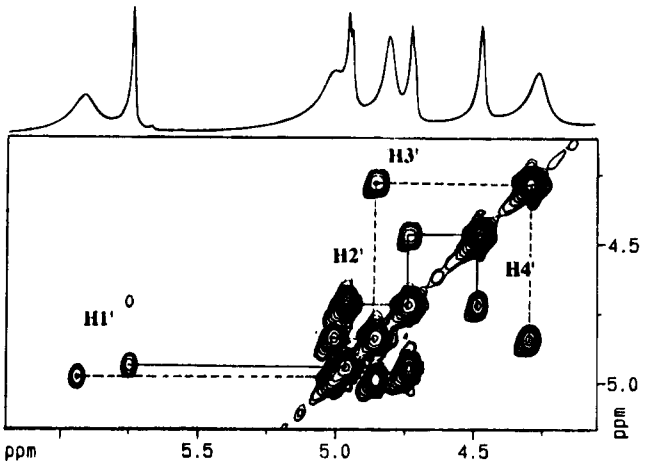

Figure 1. The ^1H–^1H COSY spectrum of isoG **3** (38 mM) at rt in $CDCl_3$ shows the H1′, 2′, 3′, 4′ region for nonexchangeable sugar ^1H–^1H correlations. There are 2 separate sets of resonances. Solid lines connect the isoG self-assembly's resonances while the dotted lines connect the monomer's resonances.

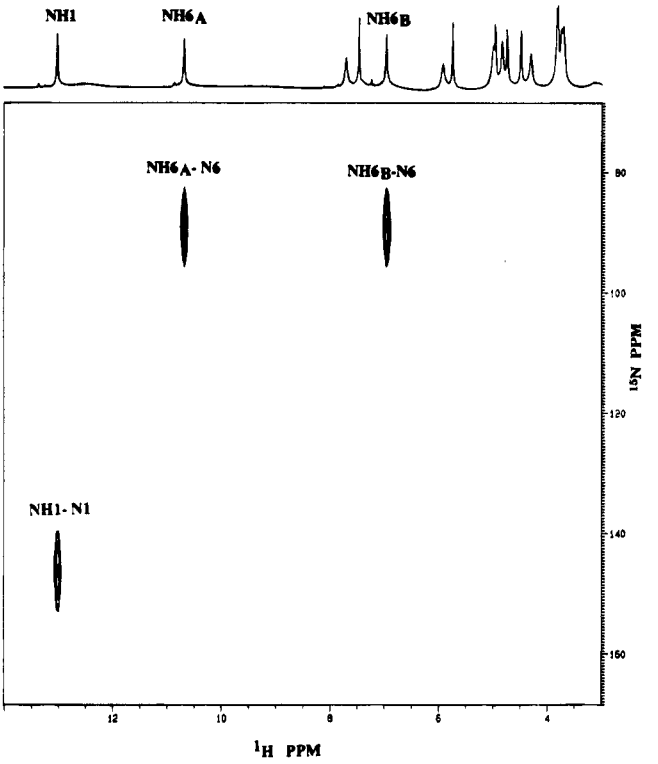

Figure 2. An ^{15}N–^1H HMQC spectrum of isoG **3** (200 mM) at rt in $CDCl_3$ shows cross peaks for exchangeable protons attached to nitrogen. A single NH imino proton is observed at 13.06 ppm. The exocyclic $C6NH_2$ amino protons, $NH6_A$ and $NH6_B$, separated by 3.6 ppm, are attached to the same nitrogen (^{15}N δ = 90.0 ppm).

tons was crucial for determining the base pairing pattern of the isoG self-assembly. The 1D ^1H NMR spectrum of isoG **3** in organic solvents showed that the three exchangeable protons had significant downfield shifts and sharp lineshapes at room temperature, indicating their involvement in strong hydrogen bonds.[28] The ^1H–^{15}N HMQC NMR experiment clearly revealed that the ^1H resonances at 10.70 ppm and 6.98 ppm were attached to the same nitrogen atom at δ = 90 ppm (Figure 2). Thus, these resonances were assigned to the two exocyclic amino protons, $C6NH_A$ and $C6NH_B$. The well-separated

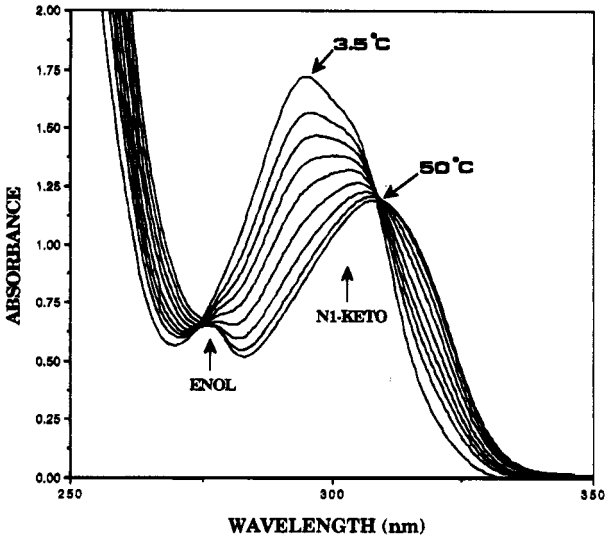

Figure 3. Temperature dependent UV spectra of isoG **3** (170 μM) in CH_3CN. At 50 °C, the absorbance maximum for the N1-keto tautomer is A_{308} = 1.22. As the temperature is decreased to 3.5 °C the keto absorbance increases in intensity and shifts to higher energy (A_{295} = 1.43). The minor enol tautomer absorbs at 278 nm. IsoG keto and enol tautomers were assigned on the basis of previous UV studies by Sepiol et al.[19]

$C6NH_A$ and $C6NH_B$ resonances ($\Delta\delta$ = 3.7 ppm) indicate that rotation about the exocyclic C6–N6 bond is slow on the NMR timescale. This slow C6–N6 bond rotation, observed even at relatively high temperatures (40 °C), is consistent with the exocyclic amine's involvement in strong hydrogen bonds. The isoG's C6 amino protons, particularly $C6NH_A$ at 10.70 ppm, are shifted far downfield compared to other nucleoside amino groups.[28] For example, the exocyclic C6 amino protons in A4 appear as a coalesced singlet at 5.86 ppm.

The $^1H-^{15}N$ HMQC experiment (Figure 2) also clearly indicates that the hydrogen-bonded isoG assembly has a single imino proton. The isoG purine could exist as either the N1 or the N3 keto tautomer. We assigned the resonance at 13.06 ppm to the N1 imino proton since this resonance shows strong $^1H-^1H$ NOEs with the exocyclic amino protons, $C6NH_A$ and $C6NH_B$ (see Figure 4). If the isoG existed as the N3 tautomer, these $NH-C6NH_A$ and $NH-C6NH_B$ NOEs would not be observed, since the corresponding interproton distances would be too far for a $^1H-^1H$ dipolar interaction.[31]

In addition to NMR evidence, UV spectra also supported the N1 keto tautomer assignment. Twenty years ago, Shugar assigned isoG's long wavelength UV band at 300 nm to the N1 keto tautomer, and the 280 nm absorbance to the enol tautomer.[20] As shown in Figure 3, the isoG derivative **3** has a predominant long wavelength band near 300 nm, indicating that the N1 keto tautomer is the major species in CH_3CN solution. A hyperchromic blue shift from 308 to 294 nm occurs when an isoG solution in CH_3CN is cooled from 50 °C to 3 °C. The increase in the N1 keto tautomer concentration as a function of temperature is consistent with enhanced isoG self-association at lower temperatures.

IsoG Tetramer Model. Both 2D NOESY and 1D NOE experiments in $CDCl_3$, d_6-acetone, and CD_3CN

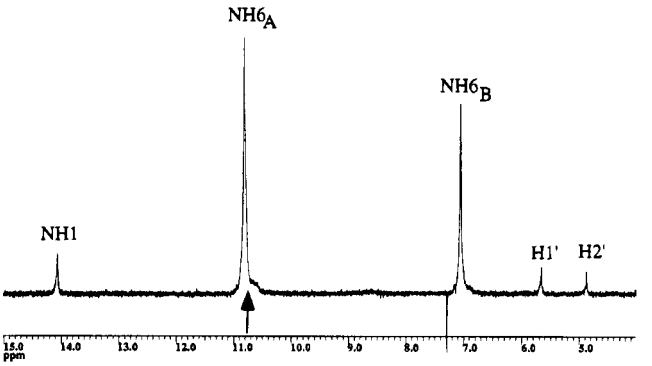

Figure 4. NOE difference spectrum for isoG **3** (38 mM) at rt in d_6-acetone containing KI (76 mM). Similar NOE difference spectra were also obtained in the absence of KI. The $NH6_A$ signal at 10.75 ppm was saturated with a 3 s irradiation time. Negative enhancements for NH1 (−3%), H1′ (−2%) and H2′ (−1%) arise from $^1H-^1H$ dipolar couplings. The large enhancement for $NH6_B$ is from both dipolar and exchange contributions.

helped determine the basic structure of the isoG assembly. First, all NOE interactions were negative for the isoG mononucleoside's major resonance set, even at 25 °C in the nonviscous organic solvents. A mononucleoside of mw 438, with $\omega\tau_c \ll 1$, should be in the extreme narrowing limit with positive NOEs.[31] Instead, the negative NOEs indicate that isoG **3** is in the slow tumbling regime ($\omega\tau_c > 1$), behaving as a relatively large molecule (mw > 1000). Hydrogen-bonded or stacked structures formed by monomer self-assembly would certainly account for the observed negative NOE interactions.[32] Second, NOEs from the purine H8 to the ribose H4′ and H5′,5″ protons reveal that isoG **3** can adopt an anti conformation about the C1–N9 glycosidic bond.[33] Third, specific NOEs between the exocyclic $C6NH_2$ amino protons and the ribose H1′ and H2′ protons confirmed isoG self-association. For example, Figure 4 shows 1D NOEs that result when the $C6NH_A$ proton is irradiated. In addition to the 1D experiment, the $C6NH_2$–H1′, H2′ NOEs were observed in a 2D $^1H-^1H$ NOESY experiment (data not shown). The $C6NH_2$–H1′, H2′ NOEs cannot be due to intramolecular interactions since the interproton distances of 6.4–9.4 Å (depending on the glycosidic angle) are much too long for $^1H-^1H$ dipolar relaxation to be observed. In fact, molecular models of isoG dimers, trimers, and tetramers show that only the C_4-symmetric tetramer **6** is consistent with the observed C6NH–H1′, H2′ NOEs. In the isoG tetramer, hydrogen bonds between the $C6NH_A$ proton and the purine N3 bring both exocyclic amino protons within 3–4 Å of the adjacent monomer's ribose H1′ and H2′ protons. Alternatively, as suggested by a reviewer, the internucleotide NH6–H1′, H2′ NOEs may arise from dipolar interactions between stacked isoG structures. We have not discounted this possiblity, although our cation titration data presented below suggests that stacking occurs only in the presence of K^+.

Our proposed model for the basic structural unit in isoG self-association is the C_4-symmetric tetramer **6** shown below. The isoG tetramer **6** is organized by an

(31) Neuhaus, D. and Williamson, M. P. *The Nuclear Overhauser Effect in Structural and Conformational Analysis;* VCH Publishers: New York; 1989; pp 63–103.

(32) C–G tetramers have negative NOEs at low temperatures: Williams, N. G.; Williams, L. D.; Shaw, B. R. *J. Am. Chem Soc.* **1989**, *111*, 7205.

(33) Rosemeyer, H.; Toth, G.; Golankiewicz, B.; Kasimierczuk, Z.; Bourgeois, W.; Kretschmer, U.; Muth, H.-P.; Seela, F. *J. Org. Chem.* **1990**, *55*, 5784.

inner and outer ring of hydrogen bonds between the Watson–Crick face of one isoG base and the complementary bottom edge of another purine unit. The inner ring's hydrogen bonds form between the imino NH1 of one monomer and the C2 carbonyl oxygen of an adjacent base, while the outer ring is composed of four $C6NH_A$–N3 hydrogen bonds. The tetramer has four nonbonded oxygen electron pairs that point toward the center of the cavity. As in the G-quartet, this central cavity is ideal for selective metal ion coordination. Our C_4-symmetric isoG tetramer is different from the structure previously proposed to be the basic building block of the poly(isoG) four-stranded helix.[20] That earlier model proposed a tetramer of C_2 symmetry, with two different N1 imino protons and two different C6 amino groups. Our ^{1}H NMR data shows only a single set of resonances and is more consistent with the C_4-symmetric tetramer.

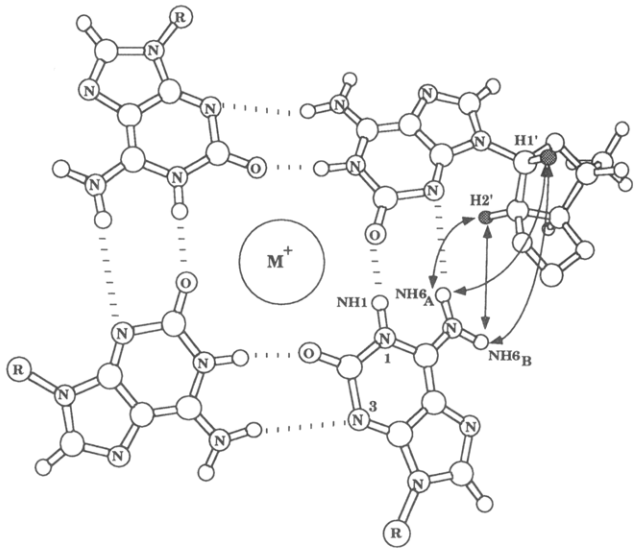

IsoG Tetramer 6

Thermodynamic Parameters of Tetramer Formation. Since the isoG monomer **3** and tetramer **6** are in slow exchange on the NMR timescale, values for the tetramer's stability constant (K_s) could be determined from integration of the ^{1}H resonances for the monomeric and tetrameric species. Since tetramer signals were evident even at low concentrations and high temperatures, it was clear that isoG tetramer formation was thermodynamically favorable. For example, NMR measurements indicate that K_s for tetramer formation is at least 10^{13} M^{-3} for a 60 μM solution of **3** in $CDCl_3$ at room temperature. Even in more polar solvents, such as CD_3CN and d_6-acetone, K_d is ca. 10^9–10^{10} M^{-3} at room temperature, as measured by varying the concentration of **3** over 0.1 to 10 mM. The temperature dependence of K_s was used to determine the free enthalpy ($\Delta H°$) and free entropy ($\Delta S°$) for isoG tetramer formation. Since its chemical shift varies the most for the monomer and tetramer, the ribose H1′ resonance was used to determine the thermodynamic parameters of self-association. Integration of ^{1}H resonances indicate that $\Delta G°$ of tetramer formation is −12.5 kcal mol^{-1} in d_6-acetone at 25 °C. The isoG tetramer's stability in d_6-acetone clearly increases with decreasing temperature, as indicated by the van't Hoff plot (ln K_s versus T^{-1}) displayed in Figure 5.

Least-squares analysis of the plotted data according to the van't Hoff equation (1) allowed $\Delta H°$ to be determinedfrom the line's slope and $\Delta S°$ to be determined from the intercept. Linear fits of data collected in 3 °C increments between 25 and 4 °C were very good, with correlation coefficients of >0.97. The van't Hoff plot reveals that isoG tetramer formation is enthalpically-driven, with $\Delta H° = -18.2$ kcal mol^{-1}. With at least eight, and possibly 12 (see below), hydrogen bonds in the tetramer's (**6**) structure, this $\Delta H°$ gives an average value of 1.5–2.3 kcal/mol per hydrogen bond in d_6-acetone. Apparently, the negative $\Delta H°$ overcomes the entropic penalty ($\Delta S°_{298} = -19.1$ eu) required for organization of four isoG monomers.

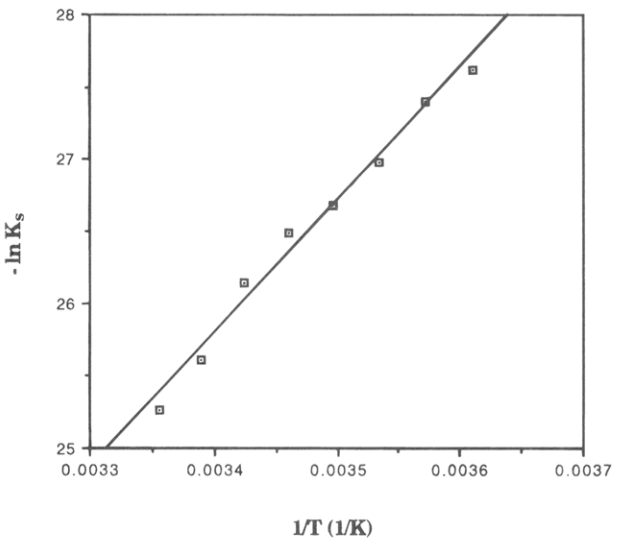

Figure 5. The van't Hoff plot for the isoG monomer–tetramer equilbrium process. The natural logarithms of the tetramer's stability constant (K_s) are plotted as a function of the inverse of the absolute temperature. The dissociation constants were determined from integration of the monomer and tetramer's separate 500 MHz ^{1}H NMR signals.

$$\ln K_s = (-\Delta H°/R)T^{-1} + (\Delta S°/R) \qquad (1)$$

Specific Ion Binding by the IsoG Tetramer. Our original goal was to build a self-assembled ionophore. The G-quartets are size-selective in coordination of monovalent cations.[6] Experiment indicates that the G-quartet binds K^+ (1.33 Å) strongly, has a weaker affinity for Na^+ (0.98 Å), and does not coordinate Li^+ (0.68 Å).[7] Since energy-minimized (MM2) structures[34] showed that the isoG tetramer's (**6**) central cavity has a 2.8–2.9 Å diameter, we anticipated that the isoG tetramer would also be size-selective in its ion-binding. The isoG tetramer's cavity has a similar diameter to that of 18-crown-6,[35] and it may be optimal for K^+ coordination. Indeed, we find that isoG self-assembly and ion coordination is highly cation dependent.

Solutions of the isoG mononucleoside **3** in d_6-acetone were titrated with LiCl, NaI, KI, and BaI_2. The ions' effect on the isoG structural equlibria was determined by integrating the seperate ^{1}H NMR resonances for the isoG monomer and oligomer. Each cation had a different effect on isoG's ^{1}H NMR spectrum (Table 3). For example, addition of LiCl completely broke up any of the tetramer that was in solution (Figure 6A). As little as 1

(34) The MM2 calculations were done using the CAChe molecular modeling program (version 3.5). CAChe Scientific, Inc , P.O. Box 500, MS 13-400, Beaverton, OR 97077.

(35) Dunitz, J. D.; Dobler, M.; Seiler, P.; Phizackerly, R. P. *Acta Crystallogr. B.* **1984**, *30*, 2733.

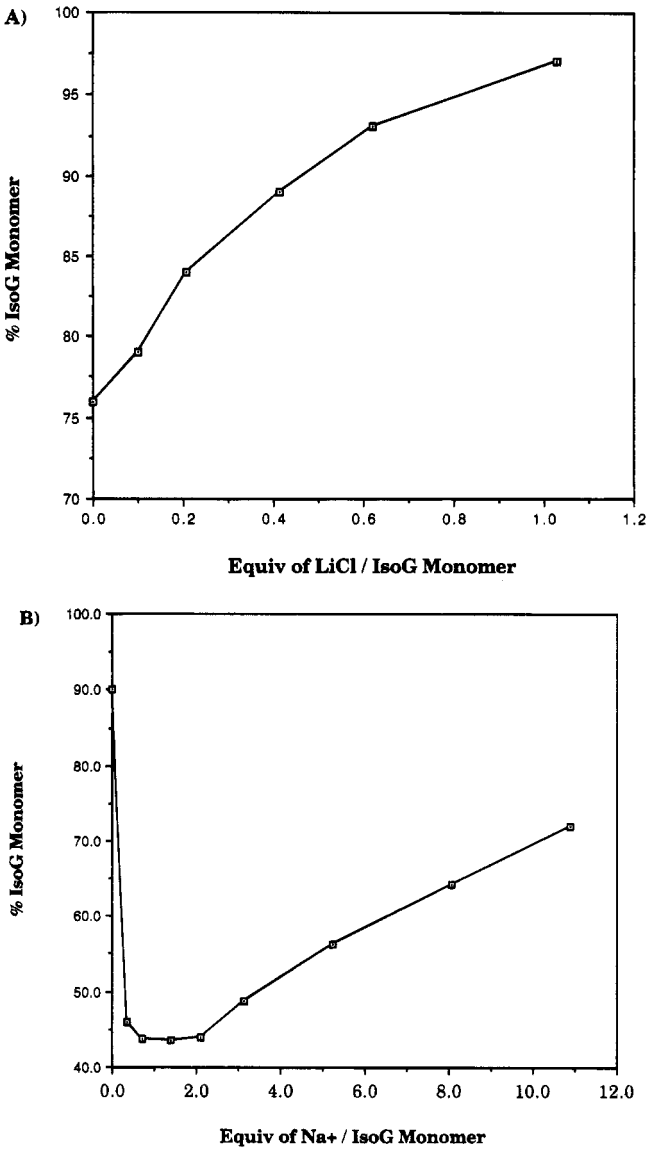

Figure 6. The percentage of isoG monomer **3** in solution is plotted as a function of the number of equivalents of monovalent cation per isoG monomer. The amount of monomer **3** and tetramer **6** were determined by integration of ^{1}H NMR spectra. The 500 MHz ^{1}H spectra were obtained using a 5 mM solution of isoG **3** at rt in d_6-acetone. (A) LiCl titration. (B) NaI titration.

equiv of Li^+ per isoG monomer shifted the equilibrium entirely to the monomer. The small Li^+ cation, with an ionic radius of 0.68 Å, cannot fit snugly into the isoG tetramer's central cavity. Instead, this electropositive ion probably coordinates the isoG O2 or N3 donor atoms and blocks hydrogen bond formation. The larger Na^+ ion, however, has a much different effect on the tetramer's stability. Unlike Li^+, small amounts of Na^+ (0.5–2.0 equiv) clearly stabilize the isoG tetramer versus the monomer (Figure 6B). Importantly, Na^+ did not cause formation of additional ^{1}H and ^{13}C NMR resonances. This suggests that higher-ordered isoG structures, such as stacked tetramers, are not formed in the presence of Na^+. Increasing amounts of NaI (2–10 equiv/monomer) destabilized the tetramer and shifted the structural equilibrium back toward the isoG monomer. In fact, saturation of the NMR solution with NaI resulted in complete formation of the isoG monomer. It is likely that Na^+ stabilizes the isoG tetramer at the lower concentrations

Table 3. Cation Dependent ^{1}H NMR Chemical Shifts for IsoG 3[a]

	chemical shift (ppm)				
resonance	no salt	LiCl	NaI	KI	BaI_2
NH1	13.07	12.06	11.10	14.06	13.92
$NH6_A$	10.8	9.35	8.16	10.75	10.83
$NH6_B$	7.20	8.80	8.16	7.17	7.27
H8	7.66 (7.99)[b]	8.17	8.17	7.98	7.98
H1′	5.88 (6.06)	6.08	5.94	5.78	5.62
H2′	5.17 (5.26)	5.43	5.27	4.99	5.02
H3′	4.95 (4.99)	5.02	4.96	4.99	4.97
H4′	4.59 (4.33)	4.30	4.33	4.44	4.51
H5′	4.01	3.85	3.80	4.12	4.17
H5″	3.86	3.85	3.80	3.94	3.92
CH_3 A	1.85 (1.58)	1.58	1.51	1.70	1.75
CH_3 B	1.49 (1.35)	1.37	1.32	1.40	1.42
tBu	0.85 (0.80)	0.81	0.72	0.89	0.87
SiMe A	0.05	−0.01	−0.05	0.14	0.11
SiMe B	0.03	−0.02	−0.06	0.12	0.13

[a] Recorded at 400 MHz in d_6-acetone @ 298 K. All samples contained excess salt. [b] Values in parentheses are for the isoG monomer **3** species.

via ion–dipole interactions. Additional Na^+ probably disrupts tetramer formation by coordinating the monomer's O2 and N3 hydrogen bond acceptor atoms.

The K^+ ion causes the most dramatic change in isoG's ^{1}H NMR spectrum. Addition of KI to a solution of isoG **3** in d_6-acetone results in disappearance of both the monomer and tetramer, with complete formation of a single, new oligomer. The K^+ titration causes some significant ^{1}H and ^{13}C chemical shift changes for the isoG multimer (Tables 2 and 3). For example, the NH1 imino proton shifts further downfield by 1 ppm to 14.06 ppm, and the nonexchangeable H8 shifts downfield by 0.32 ppm, while the ribose H1′ resonance shifts upfield by 0.10 ppm. These chemical shift changes suggest a structural modification upon K^+ binding. Indeed, the titration data shows that a 1:8 K^+ to isoG monomer stoichiometry results in a complete change in the ^{1}H NMR spectrum (Figure 7). The isoG monomer, tetramer, and K^+-octamer are all in fast exchange when there is less than 0.125 equiv of K^+ in solution (Figure 7B). Upon addition of 0.125 equiv or more of K^+ (Figure 7, parts C and D), only a single set of new ^{1}H NMR resonances are observed, even at temperatures as low as −45 °C. This unique stoichiometry is consistent with a C_{4h} symmetric isoG-K^+ octamer formed by face-to-face stacking of two isoG tetramers. The octacoordinate K^+ would be bound between the two tetramers. Such a sandwich geometry is observed in the X-ray crystal structures of stacked G-quartets in DNA oligonucleotides.[10a,i]

Interestingly, when substoichiometric amounts of BaI_2 are added to an isoG solution, three separate species, all in slow exchange at 25 °C, are observed in the ^{1}H NMR spectrum (data not shown). When more than 1/8 of an equivalent of Ba^{+2} per isoG monomer is added to the solution a new single set of resonances are observed. As for K^+, this NMR titration data is consistent with formation of a C_{4h} symmetric isoG-Ba^{+2} octamer. The isoG-Ba^{+2} octamer is, however, kinetically more stable than the isoG-K^+ octamer since the octamer and tetramer are in slow exchange. The divalent Ba^{+2} (1.34 Å) dissociates slower than K^+ (1.33 Å) from the isoG ionophore's octahedral oxygen cage.

Variable temperature ^{1}H NMR (−30 to 85 °C) in CD_3CN demonstrated the extraordinary stabilization provided by K^+ coordination of isoG. Without K^+, the isoG tetramer melts between 50–60 °C, with the hydrogen

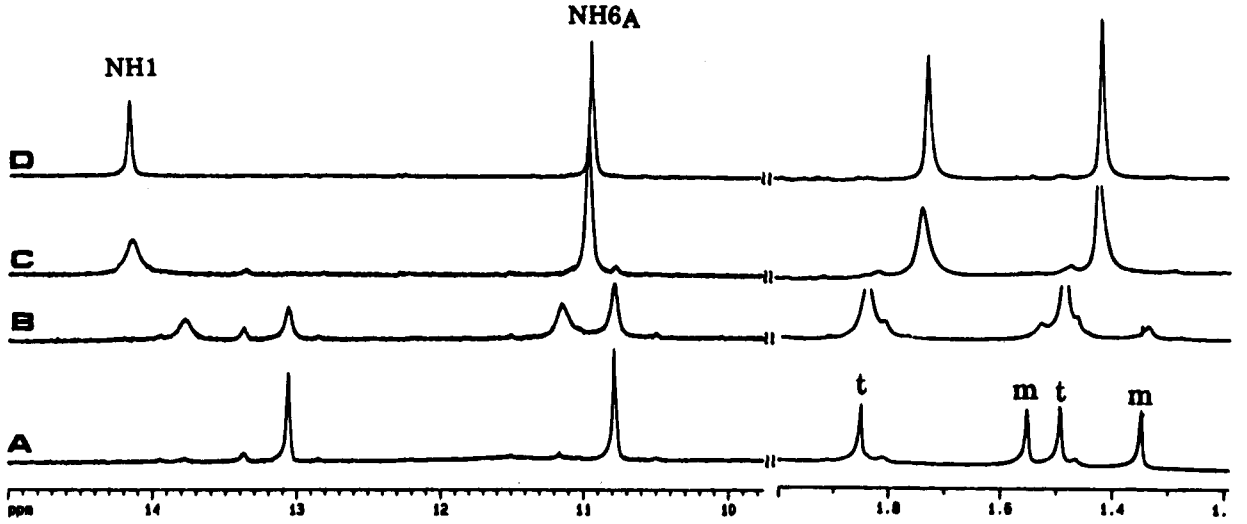

Figure 7. Regions of the 500 MHz ^{1}H NMR spectra of isoG **3** (2.5 mM) in d_6-acetone at 25 °C are shown with varying amounts of KI. The signals correspond to the imino NH1 (13.06–14.06 ppm) and amino $NH6_A$ resonances (10.80 ppm), as well as the nonexchangeable acetonide CH_3 groups (between 1.35 and 1.85 ppm). (A) Without added KI. The CH_3 groups for monomeric isoG **3** are labeled m, while the isoG tetramer's peaks are labeled t. (B) With 0.0625 equiv of KI per isoG monomer. (C) 0.125 equiv of KI per monomer (0.125 equiv). (D) With 1 equiv of KI per isoG monomer.

Table 4. NOE Enhancements for isoG 3 in the Presence of Excess Na^+ and K^+ [a]

	% NOE	
NOE[b]	KI	NaI
NH1–$NH6_A$	−5	*c*
NH1–$NH6_B$	−6	–
$NH6_B$–$NH6_A$	−46	–
$NH6_B$–NH1	−4	–
$NH6_A$–H1′	−6	–
$NH6_A$–H2′	−5	–
$NH6_B$–H1′	−5	–
$NH6_B$–H2′	−2	–
H8–H1′	−2	+2
H8–H2′	−2	+4
H1′–H2′/H3′	−1	+1
H1′–H4′	−1	+1

[a] Determined from 1D NMR in d_6-acetone @ 293 K. [b] The first proton in the pair was the irradiated resonance. [c] Exchangeable protons are not observed at room temperature.

bonded NH1 and NH6 protons completely broadened into the baseline at 40 °C. With 2 equiv of KI per isoG tetramer, however, the isoG octamer is the only observable species, even at temperatures as high as 85 °C. Even at these high temperatures distinct ^{1}H resonances are still observed for a single NH1 imino proton at 14.06 ppm and two $C6NH_2$ amino protons at 10.73 and 7.12 ppm, respectively.

One-dimensional NOE experiments, in the presence of different monovalent cations, also reveal the cation-dependent isoG association. Thus, the global correlation time (τ_c) for the isoG species is sensitive to the cation additive. As mentioned before, a mononucleoside of mw 438, with $\omega\tau_c \ll 1$, should be in the extreme narrowing limit with positive NOEs.[31] All isoG NOEs are negative, however, in the presence of K^+. The negative NOEs indicate that the isoG-K^+ octamer is in the slow tumbling regime ($\omega\tau_c > 1$), behaving as a large molecule. When excess Na^+ (>15 equiv/monomer) is present, however, isoG monomer **3** has positive NOEs in d_6-acetone (Table 4).

Chemical shifts are not the only NMR indication that K^+ stabilizes the isoG tetramer. For instance, $^3J_{HH}$ coupling constants are also cation dependent. Apparently, the isoG sugar conformation is cation-sensitive, with the ring being much more rigid in the presence of K^+. For instance, with K^+ present both $^3J_{H1',H2'}$ and $^3J_{H3',H4'}$ are < 1 Hz, indicating a narrow pseudorotational angle of $P = 255–265$ °C, with a sugar pucker between C4′-endo and O4′-endo.[36] With excess Na^+, however, $^3J_{H1',H2'}$ and $^3J_{H3',H4'}$ are 2.7 Hz and 2.3 Hz, respectively. Since $^3J_{H1',H2'}$ and $^3J_{H3',H4'}$ can never be simultaneously 2–3 Hz, according to Altona;[36] there must be conformational averaging over a wider pseudorotation range of $P = 216–324$ °C for the monomer's sugar ring in the presence of Na^+.

Lastly, isoG (**3**) also associates in the gas phase. FAB mass spectrometry of an isoG-K^+ solution (glycerol matrix) gave strong dimer peaks (mw 875.5, 45–50% of M^+), as well as signals for K^+-isoG trimer (mw 1352.1, 0.5% of dimer), and K^+-tetramer (mw 1787.7, 1% of dimer). Softer ionization methods, such as electrospray, may allow for better observation of isoG aggregation in the gas phase. Such studies are ongoing.

Comparison of IsoG Tetramer with G-Quartet. The K^+-stabilized isoG assembly is remarkable in that one symmetrical structure is formed. For example, we compared isoG-K^+ self-assembly with that for the guanosine (G) analog **5**. The NH1 imino region of the G analog's ^{1}H NMR spectrum is shown in Figure 8. Without K^+, the G mononucleoside shows two separate NH1 imino resonances. As K^+ is incrementally added, the ^{1}H NMR spectrum changes dramatically, with disappearance of the two original imino proton signals, and formation of new resonances. Eventually, at least six different NH1 imino protons are formed in the presence of relatively small amounts of K^+ (1 equiv/monomer). Such a complex ^{1}H NMR spectrum, with numerous separate NH1 imino resonances, clearly indicates that more than one G macrostructure exists on the NMR timescale. In addition, these G-K^+ structures are not nearly as stable as the isoG-K^+ octamer. For instance, heating the G-K^+ sample above 45 °C shifted the equilibrium entirely back to the G monomer.

(36) Rinkel, L. J.; Altona, C. *J. Biomol. Struct. Dyn.* **1987**, *4*, 621.

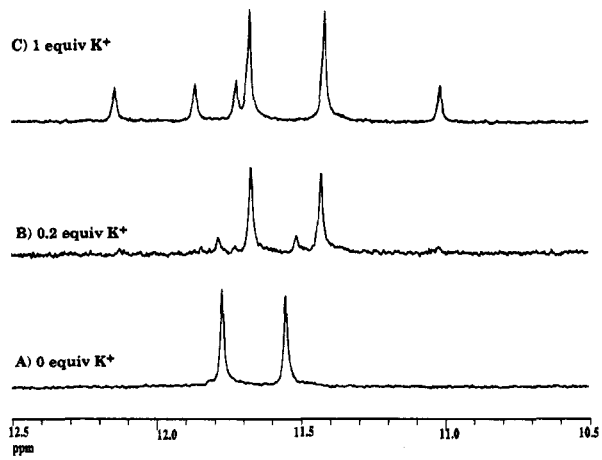

Figure 8. The NH1 imino region of the 500 MHz ^{1}H NMR spectra of the tBDMS-guanosine acetonide **5** (10 mM) in CD_3CN at 25 °C in the presence of varying amounts of KI. (A) Without added KI. (B) With 0.2 equiv of KI. (C) with 1 equiv of KI added. At least six separate NH1 imino protons are observed under these conditions.

Scheme 2

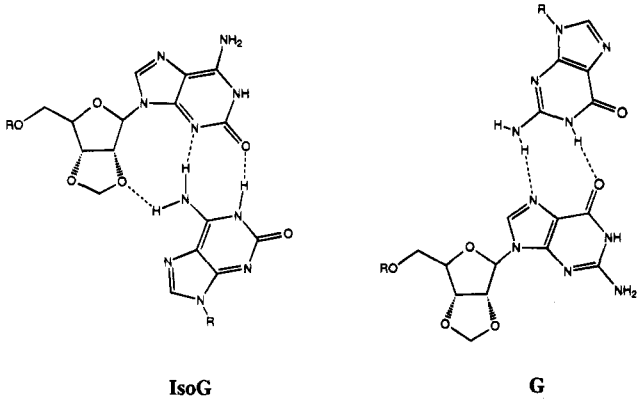

IsoG's self association is similar to that for guanosine (G),[7-9] inosine,[37] and folic acid,[38] which also have matching hydrogen bond donor and acceptor groups that enable tetramer formation. Our data, however, show that isoG forms self-assemblies that are much more stable than the corresponding G structures. Comparison of the MM2 energy-minimized structures for an isoG tetramer **6** and a G-quartet reveal why isoG self-association may be favored (Scheme 2). First, the isoG three-atom acceptor unit (O2–C2–N3), on the purine's bottom face, has a more favorable hydrogen bond geometry than the G-quartet's 4-atom Hoogsteen acceptor (N7–C5–C6–O6).[39] Hydrogen bonds are neccesarily nonlinear in the G-quartet. In contrast, the isoG tetramer's hydrogen bond angles are close to 180°. Second, and perhaps of greater importance than hydrogen bond angle, is the ability of the isoG's exocyclic $NH6_B$ proton to hydrogen bond with a ribose O2′ atom in an adjacent monomer. Such internucleoside sugar–base hydrogen bonds are not possible, however, in the G-quartet (**1**). In the G-quartet, the $NH6_B$ proton is solvent-exposed and inaccessible for internucleoside hydrogen bonding. Thus, isoG's four internucleoside $NH6_B$–O2′ base–sugar hydrogen bonds may provide enthalpic stabilization that is unavailable for the G-quartet.

In summary, isoG (**3**) uses complementary hydrogen bonds to self-assemble into a C_4 symmetric tetramer (**6**). These isoG tetramers form even in high-dielectric organic solvents. Two isoG tetramers, in turn, can coordinate K^+ and Ba^{+2} to form extremely stable octamers in solution. The isoG tetramer's extraordinary structural stability and its selective cation binding affinity are remarkable for such a noncovalent assembly made from mononucleosides. The synthesis of other self-assembled ionophores is underway.

Experimental Section

General. All synthetic reactions were done under an inert atmosphere using freshly distilled and dried solvents. TLC was performed on Kieselgel 60 F_{254} silica-coated glass plates and visualized by ethanol/sulfuric acid charring. Flash chromatography was performed using thick-walled glass columns and Kieselgel 60 brand silica gel (230–400 mesh). LiCl, NaI, KI, and BaI_2 were recrystallized and dried under vacumn before being used in titration experiments. Solvents used for NMR spectroscopy were 99.0–99.9% deuterium enriched and were used without furthur purification. All samples were degassed by repeated freeze-thaw cycles prior to the NMR experiments. The NMR spectra were obtained on a Bruker AM-400 or a Bruker AMX-500 spectrometer and are reported in ppm relative to internal TMS or the nondeuterated solvent peak. Spin multiplicities are reported as singlet (s), doublet (d), triplet (t), quartet (q), doublet of a doublet (dd), or multiplet (m), and coupling constants are given in hertz (Hz). IR spectra were recorded on a Nicolet 5DXC FT-IR spectrometer. Mass spectral data were obtained on a Fenningan 3200 twin EI and CI quadrupole mass spectrometer.

2′,3′-*O*-Isopropylideneisoguanosine. To a solution of isoguanosine[26] (1.00 g, 3.50 mmol) in anhydrous acetone (100 mL) were added 2,2-dimethoxypropane (2.9 g, 27.8 mmol) and *p*-toluenesulfonic acid (0.17 g, 0.89 mmol). After stirring at rt for 30 min, TLC indicated that the reaction was complete. The reaction mixture was concentrated to 10 mL, diluted with CH_2Cl_2 (50 mL), and washed with a 0.1 M KH_2PO_4/KOH solution, pH 7.0 (50 mL). The organic layer was dried over K_2SO_4 and concentrated *in vacuo* to give 0.90 g of a white powder. The crude product was used without purification in the next step. ^{1}H NMR (200 MHz; d_6-DMSO): 7.95 (s, 1H, H8); 7.70 (bs, 2H, $NH6_A$ and $NH6_B$); 5.86 (d, $J_{1',2'}$ = 3.4 Hz, 1H, H1′); 5.18 (dd, $J_{2',3'}$ = 6.0 Hz, $J_{1',2'}$ = 3.4 Hz, 1H, H2′); 4.88 (dd, $J_{2',3'}$ = 6.0 Hz, $J_{3',4'}$ = 2.2 Hz, 1H, H3′); 4.16 (m, 1H, H4′); 3.53 (m, 2H, H5′, H5″); 1.52 (s, 3H); 1.30 (s, 3H).

5′-(*tert*-Butyldimethylsilyl)-2′,3′-*O*-isopropylideneisoguanosine (3). To a solution of the crude 2′,3′-*O*-isopropylidene-isoG (0.88 g, 2.72 mmol) and NEt_3 (0.55 g, 5.45 mmol) in anhydrous CH_2Cl_2 (20 mL) was added a solution of *tert*-butyldimethylsilyl chloride (0.55 g, 3.66 mmol) in CH_2Cl_2 (5 mL). The mixture was allowed to stand at rt for 6 h. TLC analysis (10:1 CH_2Cl_2/MeOH) showed two major spots, corresponding to the desired product **3**, and to the N2, O5′-disilylated material. The reaction mixture was diluted with CH_2Cl_2 (25 mL) and washed with 0.1 N HCl (3 × 25 mL) and H_2O (1 × 50 mL) and concentrated *in vacuo*. The crude solid was triturated with hexane to give a **3** as an analytically pure white solid (0.64 g, 54%). ^{1}H NMR (200 MHz; d_6-DMSO): 7.89 (s, 1H, H8), 5.91 (d, $J_{1',2'}$ = 3.4 Hz, 1H, H1′); 5.24 (dd, $J_{2',3'}$ = 6.0 Hz, $J_{1',2'}$ = 3.4 Hz, 1H, H2′); 4.88 (dd, $J_{2',3'}$ = 6.0 Hz, $J_{3',4'}$ = 2.2 Hz, 1H, H3′); 4.13 (m, 1H, H4′); 3.75 (m, 1H, H5′); 3.69 (M, 1H, H5″); 1.52 (s, 3H); 1.30 (s, 3H). For ^{1}H NMR spectral data in different solvents see Tables 1 and 3 in the text. For ^{13}C NMR data in different solvents see Table 2. MS (FAB, sulfolane matrix) 438 (M^+, 100%), 460 ($M^+ + Na^+$, 24%), 476 ($M^+ + K^+$, 91%); (FAB, glycerol matrix) 438 ($M^+ + H^+$, 100%), 476 ($M^+ + K^+$, 100%); 876 ($2M^+ + H^+$, 35%), 914 ($2M^+ + K^+$, 12%), 1352 ($3M^+ + K^+$, 0.4%), 1790 ($4M^+ + K^+$, 1%). HRMS

(37) Howard, F. B.; Miles, H. T. *Biochemistry* **1982**, *21*, 6736.
(38) Ciuchi, F.; Nicola, G. D.; Franz, H.; Giovanni, G.; Mariani, P.; Bossi, M. G. P; Spada, G. P. *J. Am. Chem. Soc.* **1994**, *116*, 7064.
(39) (a) Schuster, P.; Zundel, G.; Sandorfy, C. *The Hydrogen Bond*; North Holland Co.: New York, 1976, 403. (b) Jeffrey, G. A.; Saenger, W. *Hydrogen Bonding in Biological Systems*; Springer-Verlag: New York, 1991, pp 103–110.

calcd for $C_{19}H_{32}N_5O_5Si$ 438.2095 (M^+), found 438.2099. IR 3418 m, 3100 b, 2956 s, 2768 m, 1681 s, 1606 s. UV 308, 252, 208 nm.

5′-(*tert*-Butyldimethylsilyl)-2′,3′-*O*-isopropylidene-adenosine (4) and 5′-(*tert*-Butyldimethylsilyl)-2′,3′-*O*-isopropylidene guanosine (5). The A **4** and G **5** analogs were prepared in the same manner as described for the isoG **3**. The A **4** was recrystallized from hexane/CH_2Cl_2 to give colorless needles. The G **5** analog, instead, precipitated from hexane/CH_2Cl_2 to give an amorphous white solid. Characterization of A **4**: ^{1}H NMR (200 MHz, $CDCl_3$): δ 8.41 (s, 1H, H2), 8.09 (s, 1H, H8), 6.20 (s, 1H, H1′), 5.86 (s, 2H, C6NH_2), 5.26 (d, 1H, H2′, J = 6.1 Hz), 4.98 (d, 1H, H3′, J = 6.1 Hz), 4.45 (m, 1H, H4′), 3.87 (AB q, 1H, H5′, J = 10.5, 6.0 Hz), 3.78 (AB q, 1H, H5″, J = 10.5, 6.0 Hz), 1.67 (s, 3H), 1.47 (s, 3H), 0.90 (s, 9H, t-Bu), 0.07 (s, 6H, Me_2Si). MS (FAB, sulfolane matrix) 422 (M^+, 100%), 460 ($M^+ + K^+$, 20%).

Characterization of G **5**: ^{1}H NMR (200 MHz, $CDCl_3$): δ 12.00 (bs, 1H, NH1), 7.89 (s, 1H, H8), 6.38 (bs, 2H, C2NH_2) 5.98 (s, 1H, H1′), 5.20 (d, 1H, H2′, J = 6.0 Hz), 4.90 (d, 1H, H3′, J = 6.0 Hz), 4.37 (m, 1H, H4′), 3.80 (m, 2H, H5′, H5″), 1.60 (s, 3H), 1.37 (s, 3H), 0.92 (s, 9H, t-Bu), 0.04 (s, 6H, Me_2-Si). MS (FAB, sulfolane matrix) 438 (M^+, 100%), 476 ($M^+ + K^+$, 36%).

NMR Spectroscopy. One-Dimensional (1D) NMR Experiments. The 1D ^{1}H spectra were recorded on a Bruker AMX-500 NMR spectrometer. Spectra recorded in CD_3CN, $CDCl_3$ CD_3OD, and d_6-DMSO solvents were referenced internally to the signals of the solvent's residual ^{1}H peak. Steady state NOE measurements were performed at 298 K on a Bruker AM-400 NMR spectrometer. A total of 320 transients were accumulated with alternate blocks of 32 on-resonance and 32 off-resonance pulses using an irradiation period of 3.0 s and a relaxation delay of 9.0 s. NOE difference spectra were obtained by subtracting the off-resonance spectra from the on-resonance spectra.

Two-Dimensional (2D) NMR Experiments. All 2D NMR experiments were performed on a Bruker AMX-500 NMR spectrometer using TPPI quadrature detection (Redfield, A.; Kunz, S. D. *J. Magn. Reson.* **1975**, *19*, 250−254) . Data were typically processed by zero-filling in the t1 domain to give 2K × 1K matrices, which were then apodized with a sine-bell squared filter function in both dimensions prior to Fourier transformation.

^{1}H−^{1}H Correlation Experiments. The 2D COSY experiment on isoG **3** (38 mM) in $CDCl_3$ (0.400 mL) at 298 K was recorded in the magnitude mode with 2048 data points in the t_2 dimension and a spectral width of 8620 Hz. The other acquisition parameters for the COSY experiment included 700 t_1 experiments, 32 acquisitions per experiment, and a relaxation delay of 3.0 s. The 2D NOESY experiments on isoG **2** (38 mM) were done in CD_3CN (0.400 mL), with and without saturated KI (78 mM, 2 equiv K^+/isoG monomer). The experiments were done at 233 K using the standard pulse sequence (90°-t_1-90°-t_m-90°-t_2)[30] with a 300 ms mixing time. NOESY experiments were also performed at 298 K using 200 and 300 ms mixing times. The data were collected with a t_2 spectral width of 7812 Hz, 2048 data points for each FID, and 64 transients for each of the 512 t_1 experiments with a 4.0 s relaxation delay.

HMQC Experiments. The ^{1}H−^{13}C HMQC experiments on isoG **2** (200 mM) in $CDCl_3$ (400 uL) at 298 K were recorded using the pulse sequence of Bax and Subramanian.[29] The data were collected at a ^{13}C frequency of 125.77 MHz with a 7575 Hz spectral width in the t_2 dimension. A total of 2048 data points were collected in the t_2 dimension, 338 t_1 values were collected for each data set, and 90 transients were collected for each of the 338 t_1 values using a 3.0 s relaxation delay. The natural abundance ^{1}H−^{15}N HMQC experiments on isoG **3** (200 mM) in $CDCl_3$ (400 μL) at 298 K were also performed using the pulse sequence of Bax and Subramanian.[29] An ^{15}N frequency of 50.69 MHz was used with a 7812 Hz spectral width in the t_2 dimension. A total of 1024 data points were collected in the t_2 dimension; 180 transients were collected for each of the 180 t_1 values using a 3.0 s relaxation delay.

Determination of Thermodynamic Parameters for isoG Tetramer Formation. Solutions of isoG mononucleoside **3** were made up in various solvents. Integration of the ^{1}H NMR resonances for the isoG monomer **3** and tetramer **6**, which are in slow exchange, provided concentrations of the two species. Stability constants were determined by considering only isoG monomer and tetramer using the equation K_s (M^{-3}) = tetramer/monomer^4. The K_s values were measured in 3° increments over the temperature range 253 to 293 K. Thermodynamic parameters, $\Delta H°$ and $\Delta S°$, were obtained from van't Hoff plots of $1/K_s$ vs $1/T$.

Stoichiometry of isoG Cation Binding. The stoichiometry of K^+ binding by isoG **3** was determined by 500 MHz ^{1}H NMR. A solution of isoG **3** (2.5 mM) in CD_3CN was titrated with increasing amounts of a stock KI (25 mM) solution. Conversion of the isoG monomer and tetramer to the K^+ bound isoG octamer was monitored by the disappearance of the monomer's and tetramer's ^{1}H NMR signals, and the appearance of a new set of signals due to the isoG-K^+ bound species (see Tables 2 and 3 for assignments). Similar experiments were performed with LiCl, NaCl, and BaI_2.

Temperature Dependent UV Spectra. A quartz cuvette containing isoG **3** (170 μM) in CH_3CN was sealed with parafilm. UV measurements were made at 5 °C increments over a temperature range from 3.5 to 50 °C. Measurements were done on a Milton Roy 2000 Diode Array spectrometer connected to a circulating water bath.

Acknowledgment. We thank Dr. Yiu-Fai Lam for his help with the ^{1}H−^{15}N HMQC NMR experiments and Professor Ji Wang Chern for an authentic sample of isoG. We also thank Professors Steven Benner, Philip DeShong, and Bryan Eichhorn for helpful discussions. We acknowledge financial support from the University of Maryland Graduate Research Board.

JO942082D